ResearchGate

See discussions, stats, and author profiles for this publication at: https://www.researchgate.net/publication/51841919

Accurate Time-Dependent Wave Packet Study of the Li + H-2(+) Reaction and Its Isotopic Variants

ARTICLE *in* THE JOURNAL OF PHYSICAL CHEMISTRY A · NOVEMBER 2011

Impact Factor: 2.69 · DOI: 10.1021/jp210254t · Source: PubMed

CITATIONS
10

READS
32

6 AUTHORS, INCLUDING:

Emine Aslan
Ahi Evran Üniversitesi
3 PUBLICATIONS **13** CITATIONS
SEE PROFILE

Niyazi Bulut
Firat University
40 PUBLICATIONS **278** CITATIONS
SEE PROFILE

Jesus F Castillo
Complutense University of Madrid
76 PUBLICATIONS **2,059** CITATIONS
SEE PROFILE

Octavio Roncero
Spanish National Research Council
142 PUBLICATIONS **2,821** CITATIONS
SEE PROFILE

Available from: Octavio Roncero
Retrieved on: 24 January 2016

THE JOURNAL OF PHYSICAL CHEMISTRY A

ARTICLE

pubs.acs.org/JPCA

Accurate Time-Dependent Wave Packet Study of the Li + H_2^+ Reaction and Its Isotopic Variants

E. Aslan,[†] N. Bulut,*[,†] J. F. Castillo,[‡] L. Bañares,[‡] O. Roncero,[§] and F. J. Aoiz[‡]

[†]Department of Physics, Firat University, 23169 Elazig̃, Turkey

[‡]Departamento de Química Física I, Facultad de Ciencias Químicas, Universidad Complutense de Madrid, 28040 Madrid, Spain

[§]Instituto de Física Fundamental, CSIC, C/Serrano, 123, 28006 Madrid, Spain

ABSTRACT: The dynamics and kinetics of the Li + H_2^+ reaction and its isotopic variants (D_2^+ and T_2^+) have been studied by using a time-dependent wave packet (TDWP) coupled-channel (CC) method on the ab initio potential energy surface (PES) of Martinazzo et al. [*J. Chem. Phys.* **2003**, *119*, 21]. Total initial $v = 0, j = 0$ state-selected reaction probabilities for the Li + H_2^+ reaction and its isotopic variants have been calculated from the threshold up to 1 eV for total angular momenta J from 0 to 90. Integral cross sections have been evaluated from the reaction probabilities at collision energies from threshold (≈0.2 eV) up to 1.0 eV collision. The calculated rate constants as a function of temperature show an Arrhenius type behavior in the $200 \leq T \leq 1000$ K temperature interval. It has been found to be a considerable large intermolecular kinetic isotope effect. The TDWP-CC results are in overall good agreement with those obtained applying the TDWP Centrifugal-Sudden (CS) approximation, showing that the CS approximation is rather accurate for the title reaction.

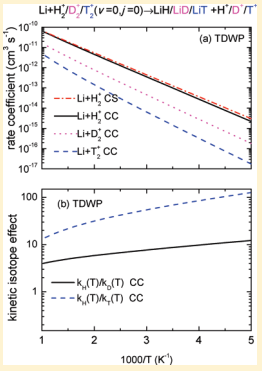

I. INTRODUCTION

The elementary chemical reaction

$$\mathrm{Li} + \mathrm{H_2^+} \rightarrow \mathrm{H^+} + \mathrm{LiH} \quad \Delta H_0^\circ = 0.217\ \mathrm{eV} \qquad (1)$$

and its reverse are considered to be of relevance in establishing the kinetic details of lithium chemistry during the evolution of the early universe in the postrecombination epoch.[1−8] Lithium chemistry in such a rarefied, dust-free environment is a lot more complex than the H, D, and He counterparts because the low ionization potential of Li-bearing species allows an effective competition between ionic and neutral processes.[2,6] In particular, the determination of LiH, LiH^+, H_2, and H_2^+ abundances in the early universe is important because these molecules act as radiative coolants that allow primordial clouds to collapse.[1,6]

Despite the small number of electrons, the LiH_2^+ system shows all the complex features of the more complicated chemical species as has been shown in a series of ab initio studies.[8−13] Global three-dimensional adiabatic potential energy surfaces (PESs) for the ground and first excited states of the LiH_2^+ system have been constructed by Martinazzo et al.[13] The potential energy surfaces are based on more than 11 000 ab initio points computed using a multireference valence bond approach[12] and extended with 600 points calculated by multireference configuration interaction (MRCI) with complete active self-consistent field reference functions and a large basis set. The first excited-state PES is relevant for reaction 1. The PES is characterized by a deep well due to dipole−charge interaction which lies 1.315 eV below the LiH + H^+ asymptote, a charge-induced dipole well 0.586 eV below the Li + H_2^+ asymptote, and a saddle point between them, which lies 0.227 eV below the LiH + H^+ asymptote. The reaction is endothermic by 0.217 eV when the zero-point energies of the reactants and products are considered ($\Delta D_e = 0.273$ eV).

There are several theoretical calculations for the title reaction[14−16] and the reverse H^+ + LiH reaction[17−21] on the first excited LiH_2^+ PES of Martinazzo et al.[13] Gogtas[14] carried out quantum calculations employing the time-dependent real wave packet (RWP) method of Gray and Balint-Kurti[22] and evaluated reaction probabilities at $J = 0$ as a function of total energy and approximate integral cross sections and thermal rate constants by a simple J-shifting approximation. Pino et al.[15] performed a quasi-classical trajectory (QCT) study of the title reaction yielding the corresponding rate constants in the temperature range of 600−4000 K. In a more recent work, RWP, flux wave packet (FWP) using the centrifugal sudden (CS) approximation, and QCT calculations for the title reaction have been reported.[16] Initial-state-resolved and total reaction probabilities for $J = 0$ and approximate FWP-CS and QCT calculations for $J \geq 0$ were presented. Besides, FWP-CS and QCT integral cross sections and rate coefficients were calculated. The calculated approximate FWP-CS and QCT rate constants as a function of temperature were shown to have an Arrhenius-type behavior.

The aim of the present work is to study the dynamics and kinetics of the Li + $H_2^+(v = 0, j = 0) \rightarrow$ LiH + H^+ reaction and its isotopic variants (with D_2^+ and T_2^+) at collision energies from threshold up to 1.0 eV using an accurate time-dependent wave

Received: October 25, 2011
Revised: November 30, 2011
Published: November 30, 2011

ACS Publications © 2011 American Chemical Society

Table 1. Parameters Used in the Wave Packet Calculations (All Distances Are Given in Å)

Reactant scattering coordinate range:	R_{min} = 0.9; R_{max} = 20.0
Number of grid points in R:	320
Diatomic coordinate range:	r_{min} = 0.4; r_{max} = 20.0
Number of grid points in r:	256
Number of angular basis functions:	240
Center of initial wave packet:	R_0 = 12.0
Initial translational kinetic energy/eV:	E_c = 0.62
Position of the analysis line:	R_∞ = 11.0
Number of Chebyshev iterations:	70 000

packet (TDWP) coupled-channel (CC) method on the ab initio PES developed by Martinazzo et al.[13] In the TDWP-CC method, the coupling between the initial and final orbital and rotational angular momenta or Coriolis coupling is implemented correctly for each value of the total angular momentum quantum number. Therefore, the present calculations go beyond the CS approximation, and they serve as a test for its validity for the title reaction. The outline of the paper is as follows: in Section II we briefly review the TDWP-CC method and the technical details of the calculations performed; Section III presents the main results and discussions; and finally, Section IV closes with some concluding remarks.

II. METHODOLOGY

We have used the TDWP-CC method developed by Roncero and co-workers[23−25] implemented in the MAD-WAVE3 code, which uses either reactant or product Jacobi coordinates to extract the state-to-state **S** matrix elements. For the reactive systems considered in this work, it has been demonstrated that it is more convenient to use reactant (r,R,γ) Jacobi coordinates given the mass combinations.[23] In these coordinates the initial wave packet that defines the initial state of the fragments $\alpha = J, M,\varepsilon,v,j$ and Ω_0 at sufficiently long distance is taken as

$$\Psi^{\alpha}(t=0) = \sum_{\Omega} W^{J\varepsilon}_{M\Omega}(\phi,\theta,\chi)\chi_{vj}(r)Y_{j\Omega}(\gamma)\left\langle R|g^{J,\varepsilon,v,j,\Omega_0}_{\Omega}(t=0)\right\rangle \tag{2}$$

where $W^{J\varepsilon}_{M\Omega}(\phi,\theta,\chi)$ is a parity-adapted basis set that depends on the ϕ,θ,χ Euler angles; $\chi_{vj}(r)$ are the ro-vibrational eigenfunctions of the AB(v,j) reactant; $Y_{j\Omega}(\gamma)$ are normalized associated Legendre polynomials; and $g^{J,\varepsilon,v,j,\Omega_0}_{\Omega}(t=0)$ is a real superposition of incoming and outgoing Gaussian functions. The radial variables r and R are described in finite grids of equidistant points, while γ is represented by Gauss−Legendre quadrature points.

The code is parallelized using the MPI library in the helicity components Ω and in the angular grid points. The initial WP is located at a sufficiently long distance R_0 so there is no influence of the interaction potential. The propagation of the WP is carried out using the Chebyshev real WP propagator, and a real absorbing function is introduced to avoid reflection at the end of the grid. The relevant parameters used in the TDWP-CC method for the three systems are given in Table 1. The parameters were chosen so the total $J = 0$ probabilities as a function of collision energy were well converged, and the same parameters were used for the calculations for $J > 0$.

The calculation of integral cross sections (ICS) as a function of collision energy for an initial ro-vibrational state v,j of the reagent molecule, $\sigma_{v,j}(E_c)$, requires summing up all the partial wave contributions of the total angular momentum J to the reaction probabilities as[26,27]

$$\sigma_{vj}(E_c) = \frac{\pi}{k^2}\frac{1}{2j+1}\sum_{J=0}^{J_{max}}(2J+1)[2\min(J,j)+1]P^J_{vj}(E_c) \tag{3}$$

where $k^2 = 2\mu_r E_c/\hbar^2$, and $P^J_{v,j}(E_c)$ is the reaction probability from the initial ro-vibrational state v,j summed over all final states as a function of collision energy, E_c, at a total angular momentum J, which can be written in terms of the **S** matrix elements[26,27]

$$P^J_{vj}(E_c) = \frac{1}{2\min(J,j)+1}\sum_{\Omega}\sum_{v',j',\Omega'}|S^J_{v',j',\Omega' v,j,\Omega}|^2 \tag{4}$$

Alternatively, the initial state-selected reaction probability $P^J_{vj}(E_c)$ can be computed using the flux operator method.[17,28]

TDWP-CC calculations for $J > 0$ are computationally very expensive, so they have been performed at selected total angular momenta values from $J = 10$ to $J = 90$ in steps of 10. An exact calculation of the $J > 0$ reaction probabilities would require us to include all possible helicity Ω projections, the maximum helicity being equal to J, and it would become very demanding. Therefore, the helicity basis that is used has been truncated, and the modulus of the helicity quantum number Ω has been restricted such that $|\Omega| \le \min(J,\Omega_{max})$, where Ω_{max} is an input parameter. The number of helicity components has been limited to $\Omega_{max} = 7$, and the convergence of the reaction probabilities with Ω_{max} will be discussed in the Results section. In addition, TDWP-CS calculations have been performed using the same program and parameters as for the TDWP-CC calculations to assess the validity of the CS approximation.

For evaluating the cross sections from eq 3 we estimate the reaction probabilities in $J \in [J_i,J_{i+1}]$ (i.e., in the intervals $J \in [0,10]$, $J \in [10,20]$, $J \in [20,30]$, and so on) via a J-shifting technique.[29] In this approach, the reaction probability for a given J value in an interval $J \in [J_1,J_2]$, is obtained as a linear interpolation[30]

$$\begin{aligned} P^J(E_c) &= \frac{J-J_1}{J_2-J_1}P^{J_1}(E_c - E^{J_2}_{shift} - E^J_{shift}) \\ &+ \frac{J_2-J}{J_2-J_1}P^{J_2}(E_c + E^{J_1}_{shift} - E^J_{shift}) \end{aligned} \tag{5}$$

where $E^{J_i}_{shift}$ is the energy threshold for J_i $(i = 1,2)$, and E^J_{shift} is obtained using the cubic expression in J

$$E^J_{shift} = AJ + BJ^2 + CJ^3 \tag{6}$$

where the A, B, and C constants are evaluated by fitting energy thresholds of the probabilities for $J = 0$, 10, 20, 30, 40, 50, 60, 70, 80, and 90 and for each reaction.

The v,j initial state-selected rate constant is calculated by averaging the corresponding ICS, $\sigma_{vj}(E_c)$, over translational energy as

$$k_{vj}(T) = \left(\frac{8k_BT}{\pi\mu_r}\right)^{1/2}\left(\frac{1}{k_BT}\right)^2\int_0^{\infty}E_c\sigma_{vj}(E_c)e^{-E_c/k_BT}dE_c \tag{7}$$

where k_B is the Boltzmann constant and μ_r is the reduced mass of the reactive system.

dx.doi.org/10.1021/jp210254t |J. Phys. Chem. A 2012, 116, 132–138

III. RESULTS AND DISCUSSION

A. Reaction Probabilities. Figure 1 displays the total reaction probabilities as a function of collision energy calculated for $J = 0$, $P^{J=0}(E_c)$, for the reaction Li + $H_2^+(v = 0,j = 0) \rightarrow$ LiH + H^+ and its isotopic variants Li + $D_2^+(v = 0,j = 0)$ and Li + $T_2^+(v = 0,j = 0)$ using the TDWP method. The reaction probabilities are compared with those calculated using a time-independent quantum mechanical (TIQM) method implemented in the ABC code.[31] In the last case, the following parameters have been used: the maximum rotational quantum number is 41; the maximum internal energy in any channel is 1.7 eV; the maximum hyperradius is 40.0 bohr; the number of log-derivative propagation sectors is 500; and the collision energy increment is 0.004 eV.

Both sets of QM calculations yield reaction probabilities in fair agreement for the three reactions considered, although some discrepancies are observable. As can be seen, the reactions show a dense structure of sharp resonances, and thus, it is difficult to obtain a perfect agreement between the two methods. Nevertheless, it is important to note that the TDWP and TIQM calculations predict the same thresholds, and the post-threshold behaviors are quite similar. This is quite reassuring because it is known that it is difficult, in general, to get well-converged TDWP results near threshold due to the need of long propagation times and well-adjusted absorbing functions.

The reaction probabilities show threshold energy values of 0.22, 0.24, and 0.25 eV for the Li + $H_2^+(v = 0,j = 0)$, Li + D_2^+ $(v = 0,j = 0)$, and Li + $T_2^+(v = 0,j = 0)$ reactions, respectively. This increase in the reaction threshold for the different isotopic variants of the reaction agrees well with the increase in endothermiticy in the reactive series when zero-point energies of reagents and products are considered. As mentioned above, a large number of very narrow peaks can be observed in both TDWP and TIQM $P^{J=0}(E_c)$ over the whole range of collision energies. The presence of resonance structures in the $P^{J=0}(E_c)$ can be expected due to the existence of deep wells in the reactant and product valleys that support a manifold of quasibound states above the dissociation limit of the LiH_2^+ molecular ion. As expected, the amplitude of the peaks in the $P^{J=0}(E_c)$ decreases with increasing collision energy since the lifetime of the quasibound states decreases as energy increases. Furthermore, as the mass of the diatom increases, the total reaction probabilities decrease near their respective thresholds, and the relative amplitude of the associated resonance peaks becomes smaller.

As we have mentioned in the Methodology section, the calculations of total reaction probabilities for $J > 0$ have been performed using a maximum value of the helicity of $\Omega_{max} = 7$. In Figure 2, the reaction probabilities for $J = 30$, $P^{J=30}(E_c)$, using $\Omega_{max} = 1, 2, 3, 4, 5, 6, 7$ for the Li + $H_2^+(v = 0,j = 0)$ reaction are compared to each other. As can be noticed, the convergence of $P^{J=30}(E_c)$ with Ω_{max} is rather quick, and even with $\Omega_{max} = 1$ good results can be already obtained. This would be an indication that the CS approximation will yield reaction probabilities in good agreement with the accurate calculations for this reactive system (see below). The reaction probabilities are fairly well-converged in the whole range of energies when the number of helicity components is limited to $\Omega_{max} = 7$.

Figure 3 shows the collision energy dependence of the total reaction probability calculated for some selected values of $J \geq 0$ employing the TDWP-CC and TDWP-CS methodologies. Similar results have been obtained for the isotopic variants D_2^+ and T_2^+. As anticipated above, there is a good agreement between

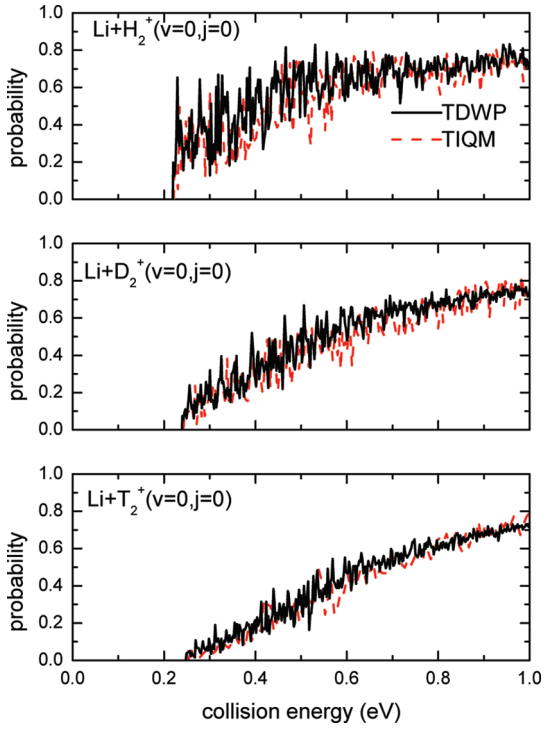

Figure 1. Total reaction probabilities as a function of collision energy at $J = 0$ for the: (a) Li + $H_2^+(v = 0,j = 0)$, (b) Li + $D_2^+(v = 0,j = 0)$, and (c) Li + $T_2^+(v = 0,j = 0)$ reactions. Black solid line: TDWP calculations. Red dashed line: TIQM calculations.

both sets of calculations at the different J values. However, the TDWP-CS method provides more oscillating reaction probabilities and, in some cases, gives rise to some overestimation, in particular at low energies or near thresholds. The reason lies in the fact that the CS approximation leads to an increase in the number of resonances and their lifetime in comparison with the CC calculation, as has been found and discussed previously for other reactive systems.[32,33] Coriolis coupling has a noticeable influence on resonances, and it plays a significant role in breaking the resonance complexes by providing an important decay mechanism of the resonance intermediates. In any case, the present results show that the CS approximation works rather well for the title reaction and its isotopic variants. This is to be expected as total reaction probabilities converge fast with Ω_{max} for this system.

As reviewed by Chu and Han,[33] the CS approximation usually fails in describing atom-molecular ion collisions, either with a barrier or a deep well. One interesting exception is the Ne + H_2^+ reaction, for which CC and CS calculations agree reasonably well.[34,35] Interestingly, the initial rotational angular momentum of the diatomic molecule is $j = 0$, so the initial helicity is $\Omega_0 = 0$, and it is conserved along the reaction in the CS approximation. In the TDWP-CC calculation the major component of the final wavepacket is expected to be $\Omega = 0$. Therefore, in classical terms, the recoiling products keep rotating in the same plane as the initial diatomic reactant. In other words, the products will rotate in a plane perpendicular to the recoil vector.

Figure 4 compares TDWP-CC total reaction probabilities for the Li + $H_2^+(v = 0,j = 0)$, Li + $D_2^+(v = 0,j = 0)$, and Li + $T_2^+(v = 0,$ $j = 0)$ reactions at $J = 10$, 30, and 60. As in the case of $J = 0$, the reaction probabilities become smaller in magnitude as the mass

dx.doi.org/10.1021/jp210254t |J. Phys. Chem. A 2012, 116, 132–138

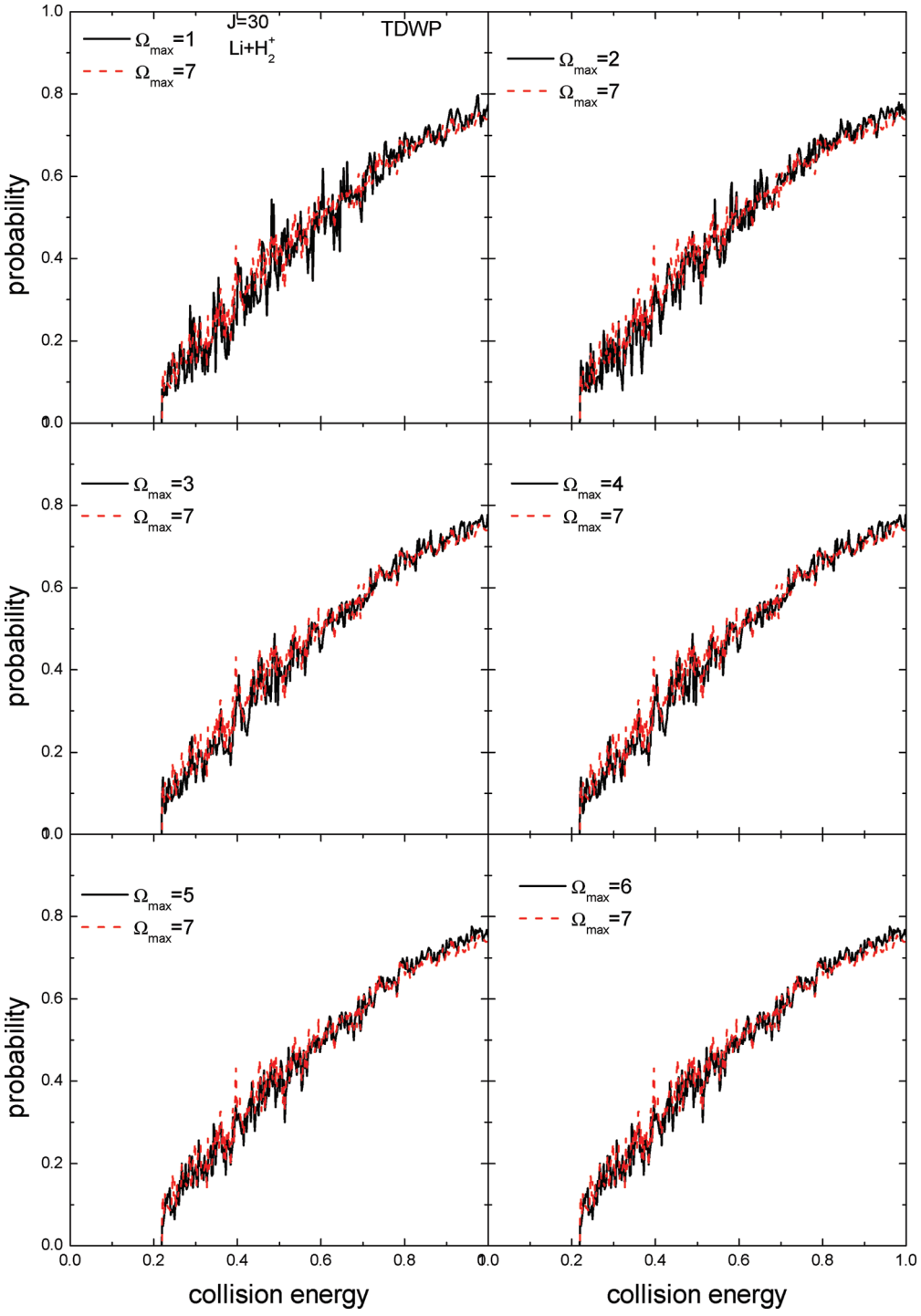

Figure 2. Total reaction probabilities as a function of collision energy for $J = 30$ and Ω_{max} =1, 2, 3, 4, 5, 6, and 7 for the Li + $H_2^+(v = 0,j = 0)$ reaction.

of the diatom increases at low and intermediate J's ($J = 10-50$), but for higher J's ($J \geq 60$) this trend is reversed to a small extent for sufficiently high collision energies. When the initial rotational angular momentum is $j = 0$, the initial helicity is $\Omega_0 = 0$, and as long as is conserved during the reaction, the CS approximation will be reliable. In fact, the major component in the CC calculation is $\Omega = 0$.

B. Excitation Functions and Rate Coefficients. Figure 5a depicts the integral cross sections (ICS) as a function of collision energy (excitation function), $\sigma(E_c)$, for the Li + $H_2^+(v = 0,j = 0)$ reaction, obtained from the TDWP-CC and TDWP-CS reaction probabilities calculated at selected values of the total angular momentum J between 0 and 90 in the collision energy range from threshold up to 1 eV. In these calculations, the J-shifting procedure described in the Methodology section has been used to interpolate for those J values where calculations were not performed. The corresponding excitation functions for the same reaction obtained in the previous FWP-CS and QCT calculations on the same PES from ref 16 are also depicted in the figure. As expected, the TDWP-CS ICSs at low collision energies are

dx.doi.org/10.1021/jp210254t |J. Phys. Chem. A 2012, 116, 132–138

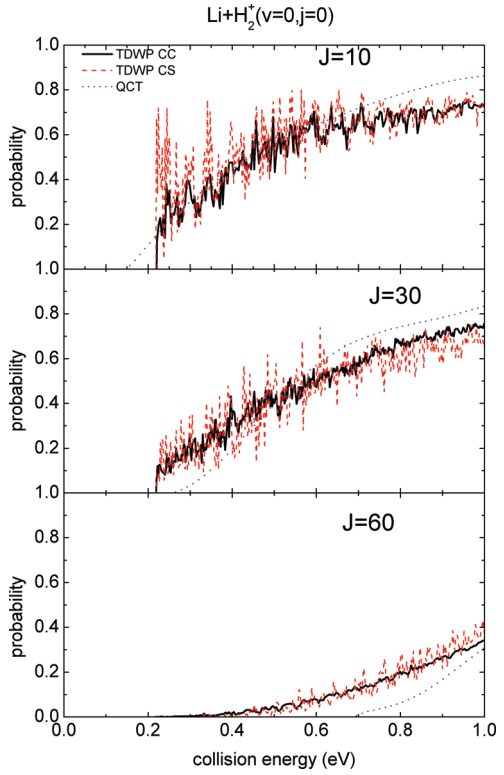

Figure 3. Total reaction probabilities as a function of collision energy for selected values of J calculated using the TDWP-CC, TDWP-CS and QCT methods for the Li + $H_2^+(v = 0,j = 0)$ reaction. Black solid line: TDWP-CC. Red dashed line: TDWP-CS. Blue dotted line: QCT (taken from ref 16).

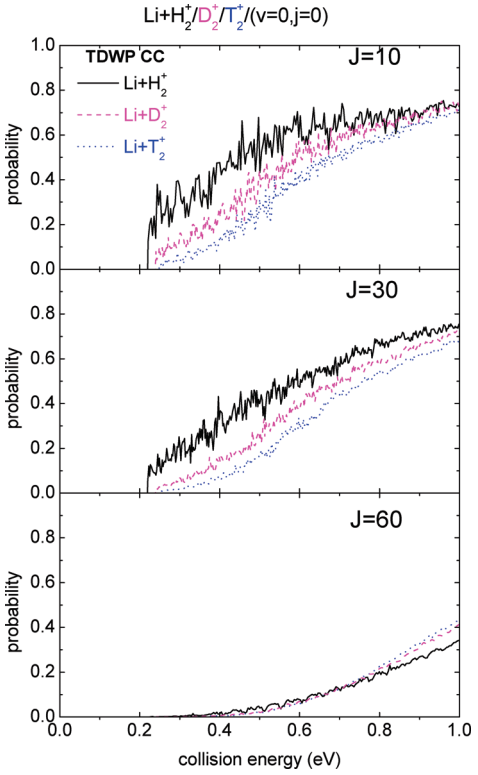

Figure 4. Total reaction probabilities as a function of collision energy for selected values of J calculated using the TDWP-CC method for the Li + $H_2^+(v = 0,j = 0)$ reaction and its isotopic variants. Black solid line: Li + $H_2^+(v = 0,j = 0)$. Magenta dashed line: Li + $D_2^+(v = 0,j = 0)$. Blue dotted line: Li + $T_2^+(v = 0,j = 0)$.

somewhat larger than those calculated using the TDWP-CC method, although they agree quite well for collision energies above 0.4 eV. The discrepancies for collision energies below 0.4 eV arise from the fact that contributions from low-J reaction probabilities to the ICS (where the largest discrepancies between TDWP-CC and TDWP-CS reaction probabilities are found) are larger in that energy range. The excitation functions show an oscillating structure that survives the summation over J. The agreement of the present TDWP-CC and TDWP-CS excitation functions with the previous Flux Wave Packet-Centrifugal Sudden (FWP-CS) calculations[16] is in general good. By contrast, the QCT calculations[16] overestimate reactivity below threshold, due to the lack of zero-point energy conservation on the products, and underestimate the ICSs above threshold because the quasi-classical method cannot account for the reactivity associated with the quantum resonances.

Figure 5b displays the TDWP-CC excitation functions for the Li + $H_2^+(v = 0,j = 0)$, Li + $D_2^+(v = 0,j = 0)$, and Li + $T_2^+(v = 0, j = 0)$ reactions. All the excitation functions exhibit a monotonic increase with increasing collision energy, and their overall magnitude noticeably diminishes as the mass of the diatomic molecule increases. Interestingly, the sharp increase in the Li + $H_2^+(v = 0,j = 0)$ excitation function after threshold is not observed in the reactions with D_2^+ and T_2^+, which show a smoother behavior. It is interesting to notice that the TDWP-CC cross sections for the Li + T_2^+ and Li + D_2^+ reactions are smaller than those obtained for the Li + H_2^+ reaction in the whole collision energy range, which indicates an isotope effect larger than one. A plausible explanation for the decreasing reactivity

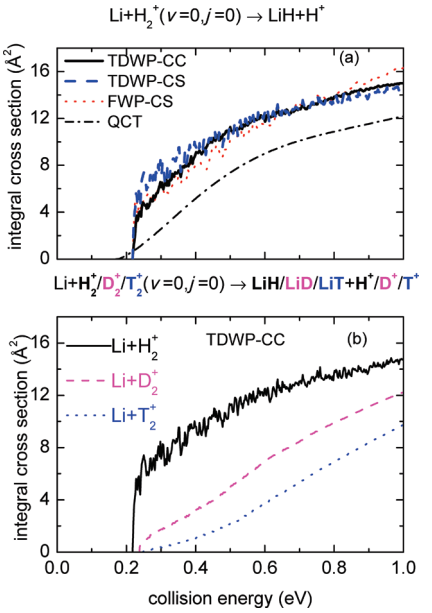

Figure 5. (a) Integral cross-section as a function of collision energy for the Li + $H_2^+(v = 0,j = 0)$ reaction. Black solid line: TDWP-CC. Blue dashed line: TDWP-CS. Red dotted line: FWP-CS. Black dotted-dashed line: QCT. The FWP-CS and QCT results are taken from ref 16. (b) TDWP-CC integral cross-section as a function of collision energy. Black solid line: Li + $H_2^+(v = 0,j = 0)$. Magenta dashed line: Li + $D_2^+(v = 0,j = 0)$. Blue dotted line: Li + $T_2^+(v = 0,j = 0)$.

dx.doi.org/10.1021/jp210254t |J. Phys. Chem. A 2012, 116, 132–138

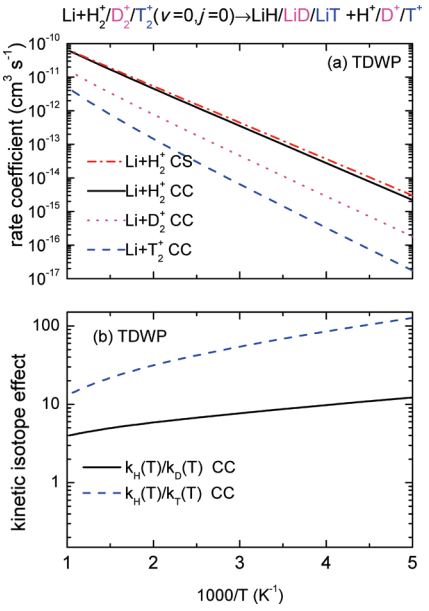

Figure 6. (a) TDWP-CC rate coefficients for the Li + $H_2^+(v = 0,j = 0)$ reaction and its isotopic variant in the 200−1000 K temperature range. (b) Intermolecular kinetic isotope effect. Black solid line: $k_H(T)/k_D(T)$. Blue dashed line: $k_H(T)/k_T(T)$.

with the mass of the hydrogen isotope can be given in terms of the effectiveness of linear momentum transfer. By inspection of the minimum energy path (see Figure 1 of ref 17), whose stationary points occur at collinear geometries, it becomes evident that formation of the products implies the stretching of the H−H (or D−D, T−T) bond. A transfer of collision energy to the vibration of the diatom is thus necessary. As it has been observed already for other reactions (see, for instance, refs 36 and 37), the lighter the isotope the more effective that energy transfer is. This result is in contrast with that found for insertion type reactions such as the $N(^2D)+H_2/D_2$ reaction with a barrier, where no significant isotope effect was found,[38] at least in the vicinity of the threshold.

The excitation functions calculated using the TDWP-CC and TDWP-CS methods have been used to evaluate specific rate coefficients for the title reaction and its isotopic variants in the temperature range 200−1000 K. These rate coefficients are shown in Figure 6a. The agreement found between the TDWP-CC and TDWP-CS rate coefficients for the Li + $H_2^+(v = 0,j = 0)$ is good in the whole temperature range and gets better as temperature increases. The rate coefficients for the reactions with D_2^+ and T_2^+ decrease substantially with respect to those of the reaction with H_2^+. This is expected considering the larger thresholds and smaller ICSs found in the excitation functions as the mass of the diatomic reagent increases. In all cases, the temperature dependence of the calculated TDWP-CC rate coefficients follows an Arrhenius behavior. A linear fit of $\ln[k(T)]$ vs $1/T$ yields activation energies of 0.22, 0.24, and 0.25 eV for the reactions with H_2^+, D_2^+, and T_2^+, respectively, in agreement with the respective reaction thresholds. The pre-exponential factors are 8.11×10^{-10}, 2.53×10^{-10}, and 9.13×10^{-11} $cm^3\ s^{-1}$, respectively.

In the previous study of the Li + $H_2^+(v = 0,j = 0)$ reaction,[16] the pre-exponential factors were somewhat smaller than that found in the present work: 4.4×10^{-10} and 6.3×10^{-10} $cm^3\ s^{-1}$ for the Flux wave packet−Centrifugal Sudden Approximation−refined−J-Shifting (FWP-CSA-RefJS) and Flux Wave Packet−Centrifugal Sudden Approximation−Separable Rotation Approximation (FWP-CSA-SRA) calculations, respectively, and 3.4×10^{-10} $cm^3\ s^{-1}$ for the QCT calculation.

Finally, Figure 6b shows the intermolecular kinetic isotope effect (KIE) defined as $k_H(T)/k_D(T)$ and $k_H(T)/k_T(T)$ calculated in the 200−1000 K temperature interval. As expected, the $k_H(T)/k_D(T)$ and $k_D(T)/k_T(T)$ (not shown) KIE ratios are comparable because the corresponding diatomic mass ratios are nearly the same. In general, the KIEs decrease moderately as temperature increases. The $k_H(T)/k_T(T)$ KIE is considerably large at low temperatures and decreases more rapidly than the $k_H(T)/k_D(T)$ and $k_D(T)/k_T(T)$ KIEs.

IV. CONCLUSIONS

In this work, first accurate TDWP-CC and approximate TDWP-CS calculations have been carried out for the Li + H_2^+ system and its isotopic variants (with D_2^+ and T_2^+) using the MAD-WAVE3 code of Roncero and co-workers[23−25] on the ab initio potential energy surface developed by Martinazzo et al.[13] Reaction probabilities have been computed using the two methods for selected values of the total angular momentum, $J = 0$, 10, 20, 30, 40, 50, 60, 70, 80, and 90. To determine integral cross sections as a function of collision energy (excitation functions), a variant of the J-shifting interpolation method has been employed, using the TDWP-CC and TDWD-CS reaction probabilities. The agreement found between the resulting excitation functions and rate coefficients using the two methods is very good, indicating that the CS approximation yields reliable results for the title reaction. As for the comparison of the excitation functions for the three isotopic variants, they show a similar behavior, i.e., increasing functions with collision energy, with an important decrease of reactivity as the mass of the diatomic reagent increases. The calculated TDWP-CC and TDWP-CS rate coefficients are in good agreement in the 200−1000 K temperature interval. The temperature dependence of the rate coefficients for the reactions studied is consistent with a simple Arrhenius model. The present calculations predict large intermolecular kinetic isotope effects for this reaction.

AUTHOR INFORMATION

Corresponding Author

*E-mail: nbulut@firat.edu.tr.

ACKNOWLEDGMENT

Financial support from the Scientific and Technological Research Council of TURKEY (TUBITAK) (Project No. TBAG-109T447) and Firat University Scientific Research Projects Unit (FUBAP-1775) is gratefully acknowledged. TDWP computations have been performed on the High Performance and Grid Computing Center (TR-Grid) at ULAKBIM/TURKEY. The authors acknowledge funding by the Spanish Ministry of Science and Innovation (grants CTQ2008-02578/BQU and Consolider Ingenio 2010 CSD2009−00038).

REFERENCES

(1) Lepp, S.; Stancil, P. C.; Dalgarno, A. *J. Phys. B: At., Mol. Opt., Phys.* **2003**, *35*, R57.

(2) Stancil, P. C.; Dalgarno, A. *ApJ.* **1997**, *458*, 543.
(3) Lepp, S.; Shull, M. *Astrophys. J.* **1984**, *280*, 465.
(4) Galli, D.; Palla, F. *Astron. Astrophys.* **1998**, *335*, 403.
(5) Palla, F.; Galli, D.; Silk, J. *Astrophys. J.* **1995**, *451*, 44.
(6) Stancil, P. C.; Lepp, S.; Dalgarno, A. *Astrophys. J.* **1996**, *458*, 401.
(7) Stancil, P. C.; Lepp, S.; Dalgarno, A. *Astrophys. J.* **1998**, *509*, 1.
(8) Bodo, E.; Gianturco, F. A.; Martinazzo, R. *Phys. Rep.* **2003**, *384*, 85.
(9) Bodo, E.; Gianturco, F. A.; Martinazzo, R.; Forni, A.; Famulari, A.; Raimondi, M. *J. Phys. Chem. A* **2000**, *104*, 11972.
(10) Bodo, E.; Gianturco, F. A.; Martinazzo, R.; Raimondi, M. *Chem. Phys.* **2001**, *271*, 309.
(11) Bodo, E.; Gianturco, F. A.; Martinazzo, R.; Raimondi, M. *J. Phys. Chem. A* **2001**, *105*, 10986.
(12) Martinazzo, R.; Bodo, E.; Gianturco, F. A.; Raimondi, M. *Chem. Phys.* **2003**, *287*, 335.
(13) Martinazzo, R.; Tantardini, G. F.; Bodo, E.; Gianturco, F. A. *J. Chem. Phys.* **2003**, *119*, 11241.
(14) Gogtas, F. *J. Chem. Phys.* **2005**, *123*, 244301.
(15) Pino, I.; Martinazzo, R.; Tantardini, G. F. *Phys. Chem. Chem. Phys.* **2008**, *10*, 5545.
(16) Bulut, N.; Castillo, J. F.; Bañares, L.; Aoiz, F. J. *J. Phys. Chem. A* **2009**, *113*, 14657.
(17) Bulut, N.; Castillo, J. F.; Aoiz, F. J.; Bañares, L. *Phys. Chem. Chem. Phys.* **2008**, *10*, 821.
(18) Cunha, W. F.; Barreto, P. R. P.; Silva, G. M.; Martins, J. B. L.; Gargano, R. *Int. J. Quantum Chem.* **2009**, *110*, 2024.
(19) Bovino, S.; Wernli, M.; Gianturco, F. A. *ApJ.* **2009**, *699*, 383.
(20) Bovino, S.; Tacconi, M.; Gianturco, F. A.; Stoecklin, T. *Astrophys. J.* **2010**, *724*, 126.
(21) Bovino, S.; Tacconi, M.; Gianturco, F. A.; Galli, D.; Palla, F. *Astrophys. J.* **2011**, *731*, 107.
(22) Gray, S. K.; Balint-Kurti, G. G. *J. Chem. Phys.* **1998**, *108*, 950.
(23) Gómez-Carrasco, S.; Roncero, O. *J. Chem. Phys.* **2006**, *125*, 054102.
(24) Zanchet, A.; Roncero, O.; González-Lezana, T.; Rodriguez-López, A.; Aguado, A.; Sanz-Sanz, C.; Gómez-Carrasco, S. *J. Phys. Chem. A* **2009**, *113*, 14488.
(25) Zanchet, A.; González-Lezana, T.; Aguado, A.; Gómez-Carrasco, S.; Roncero, O. *J. Phys. Chem. A* **2010**, *114*, 9733.
(26) Aoiz, F. J.; Sáez-Rábanos, V.; Bruno Martnez-Haya, B.; González-Lezana, T. *J. Chem. Phys.* **2005**, *123*, 094101.
(27) Alagia, M.; Balucani, N.; Cartechini, L.; Casavecchia, P.; Volpi, G. G.; Aoiz, F. J.; Banares, L.; Allison, T. C.; Mielke, S. L.; Truhlar, D. G. *Phys. Chem. Chem. Phys.* **2000**, *2*, 599.
(28) Miller, W. H. *J. Chem. Phys.* **1974**, *61*, 1823.
(29) Bowman, J. M. *Adv. Chem. Phys.* **1985**, *61*, 115.
(30) Defazio, P.; Petrongolo, C. *J. Phys. Chem. A.* **2009**, *113*, 4208.
(31) Skouteris, D.; Castillo, J. F.; Manolopoulos, D. E. *Comput. Phys. Commun.* **2000**, *128*, 133.
(32) De Fazio, D.; Castillo, J. F. *Phys. Chem. Chem. Phys.* **1999**, *1*, 1165.
(33) Chu, T.-S.; Han, K.-L. *Phys. Chem. Chem. Phys.* **2008**, *10*, 2431.
(34) Huarte-Larranaga, F.; Gimenez, X.; Lucas, J. M.; Aguilar, A.; Launay, J.-M. *J. Phys. Chem. A* **2000**, *104*, 10227.
(35) Gilibert, M.; Gimenez, X.; Huarte-Larranaga, F.; Aguilar, M.; Last, I.; Baer, M. *J. Chem. Phys.* **1999**, *110*, 6278.
(36) Aoiz, F. J.; Bañares, L.; Sáez-Rábanos, V.; Herrero, V. J.; Tanarro, I. *J. Phys. Chem. A* **1997**, *101*, 6165.
(37) Bañares, L.; Aoiz, F. J.; González-Lezana, T.; Herrero, V. J.; Tanarro, I. *J. Chem. Phys.* **2005**, *123*, 244301.
(38) Bulut, N.; Castillo, J. F.; Bañares, L.; Gogtas, F. *Chem. Phys.* **2007**, *332*, 119.